8

Instability in a Rotating Environment

8.1 Frontal Zones

Imagine a fluid whose buoyancy varies in the horizontal. You might expect that such a buoyancy distribution could not be sustained; the dense fluid would flow under the buoyant fluid, and the buoyant over the dense, until the buoyancy gradient became purely vertical.[1] On a rotating planet, though, a horizontal buoyancy gradient can be maintained by the Coriolis force. One example is the atmospheric polar front, where cold polar air flows alongside warmer mid-latitude air. Because the fluid is moving, the Coriolis force pulls it to one side (right in the northern hemisphere; left in the southern), and that force can balance the effect of the buoyancy gradient (Figure 8.1). Most major ocean currents have the same property;

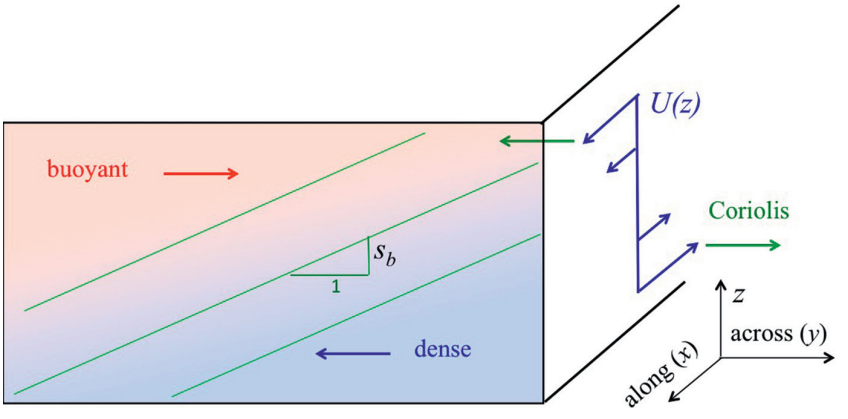

Figure 8.1 A baroclinic frontal zone in thermal wind balance. The buoyancy contrast creates a pressure gradient that is balanced by the Coriolis force. The isopycnal slope is s_b. Coordinates indicate the along-front (x) and across-front (y) directions and the vertical, z. The figure assumes that we're in the northern hemisphere and the Coriolis acceleration is therefore to the right.

[1] As in, for example, Thorpe's tilted tank experiment (Figure 4.2).

https://doi.org/10.1017/9781108640084.009 Published online by Cambridge University Press

for example, the Gulf Stream carries warm equatorial water into the cold North Atlantic.

The resulting equilibrium state is generally unstable: the Coriolis effect can maintain the density distribution in the mean, but any small disturbance will upset the balance locally. Mid-latitude weather systems result from instabilities of the polar front, while the Gulf Stream continually spins off mesoscale eddies (Figure 1.1). Those instabilities are the focus of this chapter.

Figure 8.1 describes a frontal zone. The domain of interest covers only a small part of the front, so that the buoyancy variation can be approximated as linear. With the same justification, we use Cartesian coordinates. The geographical orientation of the x and y directions is arbitrary, but for definiteness we'll imagine that the view is to the west, with south at the left. With apologies to our friends "down under," we assume we're in the northern hemisphere. The force balance is easiest to envision if we imagine a zonal flow changing direction from westward near the ground to eastward aloft. The resulting Coriolis force changes from northward to southward, balancing the buoyancy gradient.

8.2 Geostrophic Equilibrium and the Thermal Wind Balance

Our goal in this chapter is to explore equilibria and perturbations in a frontal zone. For this purpose, we'll neglect viscosity and diffusion, but retain buoyancy and re-introduce the Coriolis acceleration:

$$\vec{\nabla} \cdot \vec{u} = 0 \tag{8.1}$$

$$\frac{D\vec{u}}{Dt} = -\vec{\nabla}\pi + b\hat{e}^{(z)} + \vec{u} \times f\hat{e}^{(z)} \tag{8.2}$$

$$\frac{Db}{Dt} = 0. \tag{8.3}$$

To describe a baroclinic frontal zone like that shown in Figure 8.1, we seek an equilibrium state in which buoyancy is a function of y as well as z, and the velocity is purely zonal:

$$b = B(y, z) \; ; \quad \vec{u} = U\hat{e}^{(x)}.$$

No assumption is made about the spatial variation of U, but (8.1) requires $\partial U/\partial x = 0$, hence $U = U(y, z)$. The buoyancy equation (8.3) is satisfied automatically because there is no x-dependence for the zonal current to advect. For the same reason, the left-hand side of the momentum equation (8.2) is zero. The three components of (8.2) are then

$$\frac{\partial \Pi}{\partial x} = 0 \tag{8.4}$$

https://doi.org/10.1017/9781108640084.009 Published online by Cambridge University Press

$$\frac{\partial \Pi}{\partial y} = -fU \tag{8.5}$$

$$\frac{\partial \Pi}{\partial z} = B. \tag{8.6}$$

In order, these equations tell us that:

- The pressure, like U, can depend only on y and z.
- The meridional pressure gradient is balanced by the Coriolis force, i.e., the pressure is in geostrophic[2] balance with the current.
- The vertical pressure gradient is in hydrostatic balance with the buoyancy.

Eliminating Π between (8.5) and (8.6), we obtain the thermal wind balance:[3]

$$\boxed{f\frac{\partial U}{\partial z} = -\frac{\partial B}{\partial y}.} \tag{8.7}$$

The horizontal variation of buoyancy is referred to as baroclinicity. In the literature, you will sometimes see $\partial B/\partial y$ abbreviated as M^2 in analogy with $\partial B/\partial z = N^2$. A useful measure of the strength of the baroclinicity is the isopycnal slope:

$$s_b = -\frac{\partial B/\partial y}{\partial B/\partial z},$$

the slope of a surface on which buoyancy is uniform (Figure 8.1). Using (8.7), we can also write

$$s_b = \frac{f\partial U/\partial z}{\partial B/\partial z}.$$

8.3 The Perturbation Equations

We now linearize (8.1–8.3) by applying perturbations $\vec{u}'$, π', and b'. As always, the perturbation is incompressible:

$$\vec{\nabla}\cdot\vec{u}' = 0. \tag{8.8}$$

The linearized momentum equation is

$$\left(\frac{\partial}{\partial t} + U\frac{\partial}{\partial x}\right)\vec{u}' + \underbrace{\frac{\partial U}{\partial y}v'\hat{e}^{(x)}}_{(1)} + \frac{\partial U}{\partial z}w'\hat{e}^{(x)} = -\vec{\nabla}\pi' + b'\hat{e}^{(z)} + \underbrace{\vec{u}'\times f\hat{e}^{(z)}}_{(2)}, \tag{8.9}$$

[2] Literally "Earth turning."

[3] The name reflects the meteorological origins of the concept, but it is equally relevant in any rotating, stratified fluid.

https://doi.org/10.1017/9781108640084.009 Published online by Cambridge University Press

while the buoyancy equation becomes

$$\left(\frac{\partial}{\partial t}+U\frac{\partial}{\partial x}\right)b'+\underbrace{\frac{\partial B}{\partial y}v'}_{(3)}+\frac{\partial B}{\partial z}w'=0. \tag{8.10}$$

The braced terms in (8.9) and (8.10) have not appeared in previous models (e.g., 4.8, 4.10) where there was no ambient rotation and the mean state varied only with z. The final term in (8.9), marked (2), is the Coriolis acceleration, and can be expanded as $fv'\hat{e}^{(x)}-fu'\hat{e}^{(y)}$. The remaining new terms, (1) and (3), represent advection of the horizontal gradients of U and B by the cross-front velocity perturbation v'.

8.4 Energetics

As in section 3.10.1, we derive the equation for the perturbation kinetic energy by dotting $\vec{u}'$ onto the perturbation velocity equation which, in this case, is (8.9). The result is

$$\left(\frac{\partial}{\partial t}+U\frac{\partial}{\partial x}\right)\frac{|\vec{u}'|^2}{2}+\frac{\partial U}{\partial y}u'v'+\frac{\partial U}{\partial z}u'w'=-\vec{u}'\cdot\vec{\nabla}\pi'+b'w'+\vec{u}'\cdot(\vec{u}'\times f\hat{e}^{(z)}). \tag{8.11}$$

The final term vanishes, because the cross product is perpendicular to $\vec{u}'$. In physical terms, this reflects the fact that the Coriolis acceleration acts at right angles to the flow (e.g., to the right in the northern hemisphere). It therefore affects the *direction* of the flow but not the *magnitude*. The kinetic energy, being a measure of the magnitude, is unaffected by the Coriolis acceleration.

Rotation therefore has this property in common with stable stratification (section 4.9) and viscosity (section 5.9): it cannot, by itself, transfer energy to the perturbation. It can, however, alter the form of the perturbation such that it gains energy via the shear or buoyancy production mechanisms.

We next use (8.1) to convert $\vec{u}'\cdot\vec{\nabla}\pi'$ to $\vec{\nabla}\cdot(\vec{u}'\pi')$ and bring the second and third terms to the right-hand side:

$$\left(\frac{\partial}{\partial t}+U\frac{\partial}{\partial x}\right)\frac{|\vec{u}'|^2}{2}=-\vec{\nabla}\cdot(\vec{u}'\pi')-\frac{\partial U}{\partial y}u'v'-\frac{\partial U}{\partial z}u'w'+b'w'. \tag{8.12}$$

Applying a horizontal average and rearranging a little, we arrive at

$$\boxed{\frac{\partial}{\partial t}\overline{\frac{|\vec{u}'|^2}{2}}=-\frac{\partial}{\partial z}\overline{w'\pi'}-\frac{\partial U}{\partial z}\overline{u'w'}+\overline{b'w'}-\frac{\partial U}{\partial y}\overline{u'v'}.} \tag{8.13}$$

Most of this should look very familiar. The first and second terms on the right were described in section 3.10.1: the first is the convergence of the vertical energy flux, which vanishes when integrated in the vertical; the second is the shear production.

https://doi.org/10.1017/9781108640084.009 Published online by Cambridge University Press

The third term is the buoyancy flux that we discussed (in normal mode form) in section 4.9: it is positive (i.e., adding to the kinetic energy of the perturbation) if buoyant fluid is rising and dense fluid is falling. In the reverse case, the perturbation must do work against gravity to grow, so this term exerts a damping influence.

The fourth term is new, but it will be easily recognized as a second shear production term. Through it, the instability can exchange energy with the mean flow by advecting the horizontal shear $\partial U/\partial y$.

8.5 The Vertical Vorticity Equation

The planet's rotation can be thought of as a vorticity whose vertical component is f. Measured in an inertial reference frame, the total vorticity would be that of the flow as we measure it plus the extra contribution from the planet, a circumstance that affects the flow profoundly. In this chapter we will pay special attention to factors affecting vorticity. Since we have made the *f*-plane approximation (f = const.), the vertical component of vorticity is the most important.

The perturbation vertical vorticity is given by

$$q' = \frac{\partial v'}{\partial x} - \frac{\partial u'}{\partial y}. \tag{8.14}$$

We derive an evolution equation for q' from the x and y components of the perturbation momentum equation (8.9), namely:

$$\left(\frac{\partial}{\partial t} + U\frac{\partial}{\partial x}\right)u' + \frac{\partial U}{\partial y}v' + \frac{\partial U}{\partial z}w' = -\frac{\partial \pi'}{\partial x} + fv' \tag{8.15}$$

and

$$\left(\frac{\partial}{\partial t} + U\frac{\partial}{\partial x}\right)v' = -\frac{\partial \pi'}{\partial y} - fu'. \tag{8.16}$$

Subtracting the y derivative of (8.15) from the x derivative of (8.16), we obtain

$$\left(\frac{\partial}{\partial t} + U\frac{\partial}{\partial x}\right)q' = \underbrace{v'\frac{\partial}{\partial y}\left(\frac{\partial U}{\partial y}\right) + w'\frac{\partial}{\partial z}\left(\frac{\partial U}{\partial y}\right)}_{advection} + \underbrace{\frac{\partial U}{\partial z}\frac{\partial w'}{\partial y}}_{tilting} + \underbrace{f_a\frac{\partial w'}{\partial z}}_{stretching}. \tag{8.17}$$

The first two terms on the right-hand side describe advection of the background vorticity $-\partial U/\partial y$ by the velocity perturbations v' and w'. The third represents vortex tilting as shown in Figure 8.2a. The vertical shear of the mean flow carries y-vorticity, which is tilted toward the vertical by differences in vertical motion. The

https://doi.org/10.1017/9781108640084.009 Published online by Cambridge University Press

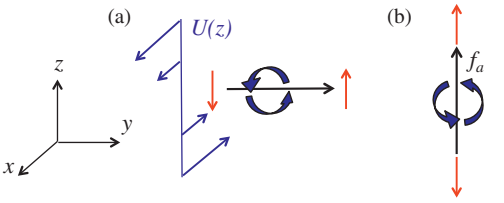

Figure 8.2 Mechanisms governing the perturbation vorticity as in (8.17). Red arrows depict the vertical velocity w'. (a) Tilting of the mean vertical shear by cross-front variations in w'. (b) Stretching of the absolute vertical vorticity by the vertical strain $\hat{w}'_z$.

final term of (8.17), illustrated in Figure 8.2b, represents vortex stretching.[4] The total vertical vorticity (that of the planet plus the mean flow, as would be measured by an observer in outer space) is written as

$$f_a = f - \frac{\partial U}{\partial y}. \tag{8.18}$$

In the final term of (8.17), that total vorticity is stretched or compressed by the vertical strain $\partial w'/\partial z$.

8.6 Analytical Solution #1: Inertial and Symmetric Instabilities

Here we consider two cases in which nothing varies in the along-front (x) direction. This eliminates advection of the perturbation by the along-front background flow, i.e., $U\partial/\partial x = 0$, an extreme simplification that enables two interesting analytical solutions, both of which are important in the Earth's oceans and atmosphere.

First, we will neglect buoyancy in order to focus on the Coriolis effect. The result is the inertial instability. In the second case we will restore buoyancy effects and thereby examine symmetric instability.

8.6.1 Inertial Instability

For zonal shear flow $u = U\hat{e}^{(x)}$ in a homogeneous fluid in a rotating environment, the equilibrium state is described by

$$\frac{\partial \Pi}{\partial x} = 0, \quad \frac{\partial \Pi}{\partial y} = -fU, \quad \frac{\partial \Pi}{\partial z} = 0, \tag{8.19}$$

[4] In case you are unfamiliar with vortex stretching, the strain $\partial w/\partial z$, when positive, causes fluid parcels to become taller and thinner. Because each parcel has vorticity f_a directed vertically, that vorticity is amplified to conserve angular momentum, like the classical example of a figure skater pulling their arms inward to spin faster. If $\partial w/\partial z < 0$, the opposite happens: the fluid parcel is compressed vertically and the vertical vorticity is reduced.

https://doi.org/10.1017/9781108640084.009 Published online by Cambridge University Press

A meridional pressure gradient maintains geostrophic balance. The pressure does not vary in x or z, and therefore (by differentiating the middle equation with respect to x or z) neither does the velocity, i.e., $U = U(y)$.

The perturbation equations are now

$$\frac{\partial v'}{\partial y} + \frac{\partial w'}{\partial z} = 0 \tag{8.20}$$

$$\frac{\partial u'}{\partial t} = -\frac{\partial U}{\partial y} v' + f v' \tag{8.21}$$

$$\frac{\partial v'}{\partial t} = -\frac{\partial \pi'}{\partial y} - f u' \tag{8.22}$$

$$\frac{\partial w'}{\partial t} = -\frac{\partial \pi'}{\partial z}. \tag{8.23}$$

The only coefficient is $\partial U/\partial y$, which varies only in the y direction; hence, we can use a normal mode solution of the form

$$v' = \hat{v}(y) e^{\sigma t + \imath m z}.$$

Note that $k = 0$ in accordance with our assumption that the perturbations do not vary in x. (Remember also that only the real part is relevant, and that corresponding expressions are used for w', u', b', and π'.) The resulting normal mode equations are

$$\hat{v}_y + \imath m \hat{w} = 0 \tag{8.24}$$

$$\sigma \hat{u} = (f - U_y)\hat{v} \tag{8.25}$$

$$\sigma \hat{v} = -f\hat{u} - \hat{\pi}_y \tag{8.26}$$

$$\sigma \hat{w} = -\imath m \hat{\pi} \tag{8.27}$$

where the subscript y indicates the derivative. These can be reduced by combining (8.24) and (8.27) to get

$$\hat{\pi} = -\frac{\sigma}{m^2} \hat{v}_y.$$

Substituting this into (8.26) along with (8.25) yields the single stability equation

$$\sigma^2(\hat{v}_{yy} - m^2 \hat{v}) = m^2 f (f - U_y)\hat{v}. \tag{8.28}$$

Notice that this equation is isomorphic with the convection equation (2.29) after the substitutions $\hat{w} \to \hat{v}$, $z \to y$, $\tilde{k} \to m$, and $B_z \to f(f - U_y)$. Making the same substitutions in the convective growth rate bound (2.34), we see that the growth rate is bounded from above by

$$\sigma < \sqrt{-\min_y \{ f(f - U_y) \}}, \tag{8.29}$$

https://doi.org/10.1017/9781108640084.009 Published online by Cambridge University Press

and instability is possible only if $f(f - U_y) < 0$ at some latitude. In other words, the relative vorticity must be *anticyclonic*, meaning in this case that $-U_y$ has sign opposite to f, and it must be greater in magnitude than f. In the northern hemisphere, for example, U must increase (become more eastward) toward the pole.

By analogy with the convective and centrifugal instabilities (section 7.8.1), inertial instability can grow wherever there is a negative local minimum in $f(f - U_y)$. The fastest-growing mode has arbitrarily small vertical wavelength and growth rate that approaches the upper bound (8.29).

Inertial Instability – Physical Mechanism

The mechanism of inertial instability is similar to the mechanisms of the convective and centrifugal instabilities described in section 7.8, but there is a slight complication. In those previous cases, the destabilizing force acted in only one direction: gravity downward, centrifugal force outward. In contrast, the Coriolis force acts in two directions, zonal and meridional, adding a new element to the process.

In the inertially unstable flow geometry considered here, the background zonal velocity at some latitude decreases with distance from the pole (Figure 8.3).

(i) Suppose a northward flow is initiated at some altitude (thick red arrow). It advects with it a negative (westward) perturbation in zonal velocity, u'.

(ii) The westward perturbation sets up a northward Coriolis force (F', thin red arrow), which accelerates the northward flow, completing a positive feedback loop.

(iii) Now here is the complication: the northward flow (red arrow) *also* experiences an eastward Coriolis acceleration (in the northern hemisphere). If that acceleration dominates, then u' is eastward and the feedback is negative. Only if the advective effect dominates, i.e., if $U_y > f$, is the net zonal acceleration westward and the flow unstable.

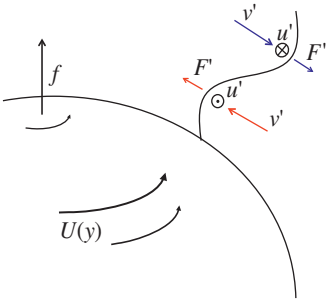

Figure 8.3 Perturbations involved in inertial instability. The meridional motion v advects the background zonal velocity to create a perturbation, F', in the Coriolis force.

https://doi.org/10.1017/9781108640084.009 Published online by Cambridge University Press

The northward motion is accompanied by southward motion at some other altitude. There, the reverse process happens (blue arrows). In the southern hemisphere, the signs are reversed in the above argument, but the criterion $f(f - U_y) < 0$ remains generally valid.

Exercise: Examine the perturbation equations and identify the terms that correspond to the three-part processes described above.

8.6.2 Symmetric Instability

We now reintroduce the frontal stratification (Figure 8.4), so that U must vary in z to maintain thermal wind balance:

$$f\frac{\partial}{\partial z}U(y,z) = -\frac{\partial}{\partial y}B(y,z). \tag{8.30}$$

We retain the assumption that nothing varies in the along-front (x) direction.

For this discussion we make two additional simplifying assumptions:

- To facilitate a normal mode solution, all mean gradients (U_y, U_z, B_y, and B_z) are assumed to be uniform, with $fU_z = -B_y$ in accordance with (8.30).
- The perturbation is *quasi-hydrostatic* in the sense that b' can be approximated by $\partial\pi'/\partial z$.[5] This assumption is easily relaxed; it merely simplifies the algebra.

With these assumptions, the coefficients of the perturbation equations (8.1, 8.9, 8.10) are all constants, and we can seek a solution using normal modes of the form

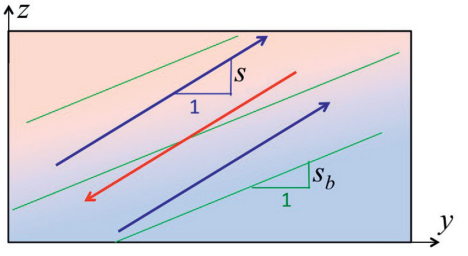

Figure 8.4 Definition sketch for symmetric instability. The thin green lines are isopycnals, with slope $s_b = -B_y/B_z$. Arrows show buoyant (red) and dense (blue) currents whose slope is $s = -\ell/m$. The flow is invariant in the along-front (x) direction.

[5] Admonition: This does *not* mean that $\hat{w} = 0$, as a look at the vertical momentum equation,

$$(\sigma + \imath kU)\hat{w} = -\hat{\pi}_z + \hat{b},$$

might suggest (cf. 8.23). Vertical motions, slow as they may be, play a critical role in the other equations by advecting the vertical gradients U_z and B_z. The assumption we make here is only that the left-hand side of (8.23) is a small difference between two large quantities $\hat{b}$ and $\hat{\pi}_z$, so we can approximate the latter as equal.

https://doi.org/10.1017/9781108640084.009 Published online by Cambridge University Press

$$u' = \hat{u} e^{\sigma t} e^{\iota(\ell y + m z)},$$

where the complex amplitude $\hat{u}$ is a constant.

The normal mode equations are now

$$\iota \ell \hat{v} + \iota m \hat{w} = 0 \tag{8.31}$$

$$\sigma \hat{u} + U_y \hat{v} + U_z \hat{w} = f \hat{v} \tag{8.32}$$

$$\sigma \hat{v} = -\iota \ell \hat{\pi} - f \hat{u} \tag{8.33}$$

$$\iota m \hat{\pi} = \hat{b} \tag{8.34}$$

$$\sigma \hat{b} + B_y \hat{v} + B_z \hat{w} = 0. \tag{8.35}$$

To express this system as an eigenvalue equation, we solve (8.31) for $\hat{w}$ and (8.34) for $\hat{\pi}$, then substitute the results into the remaining equations. This leaves us with three homogeneous equations for the three unknowns $\hat{u}$, $\hat{v}$, and $\hat{b}$. The characteristic equation is easily found:

$$\sigma^2 = \frac{\ell^2}{m^2} B_z - 2 \frac{\ell}{m} f U_z - f(f - U_y), \tag{8.36}$$

where use has been made of the thermal wind relation $B_y = -f U_z$ (8.7, 8.30).

A few abbreviations will be useful here. First, note that the wave vector components ℓ and m appear only as the ratio ℓ/m, which is minus the ratio $\hat{w}/\hat{v}$ according to (8.31). As shown in Figure 8.4, this is the slope of the planes to which motion is restricted:

$$s = -\frac{\ell}{m}.$$

The slope of the isopycnals (thin lines in Figure 8.4) is

$$s_b = -\frac{B_y}{B_z} = \frac{f U_z}{B_z}.$$

Finally, the quantity $f - U_y$ is the absolute vorticity f_a, as defined in section 8.5. With these abbreviations the characteristic equation (8.36) becomes

$$\sigma^2 = -B_z s^2 + 2 B_z s_b s - f f_a. \tag{8.37}$$

Differentiation with respect to s shows that the growth rate is a maximum when

$$s = s_b,$$

and that

$$\boxed{\sigma_{max} = |f| \left(\frac{U_z^2}{B_z} - \frac{f_a}{f} \right)^{1/2}.} \tag{8.38}$$

Exercise: Derive $s = s_b$ and (8.38) from (8.37).

https://doi.org/10.1017/9781108640084.009 Published online by Cambridge University Press

Exercise: Repeat the whole derivation without using the quasi-hydrostatic approximation. You will find that the latter is equivalent to assuming that the slopes s and s_b are small. This makes sense if you examine (8.23) and recognize that small slope implies small vertical velocity.

Remembering that B_z/U_z^2 is the Richardson number Ri, the condition for σ_{max} to be real can be written as

$$Ri < \frac{f}{f_a}. \tag{8.39}$$

For example, if there is no across-front shear, then $f_a = f$ and the condition for instability is $Ri < 1$.

A few points to consider:

- Unlike the similar condition $Ri < 1/4$ for shear instability, (8.39) is a necessary *and sufficient* condition, i.e., instability is guaranteed if the condition is satisfied.
- Like convection in an inviscid, unbounded fluid, symmetric instability has no preferred length scale (cf. section 2.2.2). The growth rate depends only on the orientation of the wave vector, and symmetric instability is therefore a broadband instability.
- The across-front shear U_y can have either a stabilizing or a destabilizing influence depending on its sign. If U_y has the same sign as f (i.e., $U_y > f > 0$ in the northern hemisphere), the across-front shear reduces the absolute vorticity f_a. From (8.38) we see that this increases the growth rate, while (8.39) shows that the criterion for Ri is relaxed. The reverse is true if U_y has sign opposite to f.
- If we reduce the buoyancy gradients to zero, we recover inertial instability as described in the previous section.

Symmetric Instability – Physical Mechanism

Recall that inertial instability grows when meridional flow advects the velocity gradient U_y, setting up a Coriolis acceleration that reinforces the original meridional flow. The only difference in the symmetric case is that the velocity gradient has a second component, U_z, that can be advected if the perturbation velocity has a vertical component. In fact, the instability can grow even if $U_y = 0$, solely by advecting the vertical shear.

Note that buoyancy has no direct effect on the fastest-growing symmetric instability. When $s > s_b$, as in Figure 8.4, the instability does work against gravity, whereas the opposite is true if $s < s_b$. For the fastest-growing symmetric instability, motion is along isopycnals ($s = s_b$) and the mode therefore exchanges no energy with the gravitational field. The energy source can only be the kinetic energy of the along-front current.

https://doi.org/10.1017/9781108640084.009 Published online by Cambridge University Press

8.7 Analytical Solution #2: Baroclinic Instability

For perturbations that vary in the along-front direction (as distinct from inertial and symmetric instability), analytical solutions are available provided that we make the set of simplifying assumptions that define a quasigeostrophic flow. The essential assumption is that the flow varies slowly relative to the Earth's rotation, i.e., on a time scale much greater than a day. The conditions for quasigeostrophy to hold are described in much more detail elsewhere, e.g., Pedlosky (1987). Here we will give only enough detail to make the approximation plausible. We will find, however, that the characteristics of the predicted instability correspond well with those of (1) mid-latitude storms and (2) oceanic mesoscale eddies.

8.7.1 The Quasigeostrophic Potential Vorticity Perturbation

The vertical component of the perturbation vorticity, introduced in section 8.5, is

$$q' = v'_x - u'_y \tag{8.40}$$

(writing partial derivatives as subscripts). Its evolution equation (8.17) is written as

$$q'_t = \underbrace{-Uq'_x}_{advection} + \underbrace{U_z w'_y}_{tilting} + \underbrace{f_a w'_z}_{stretching} . \tag{8.41}$$

We now make two critical assumptions. First, we assume that the vortex tilting effect is negligible in comparison with the stretching effect, i.e., $|U_z w'_y| \ll |f_a w'_z|$ (Figure 8.2). Second, we neglect U_y relative to f so that f_a is replaced by f.

This leaves us with the approximate vertical vorticity equation

$$\boxed{q'_t + Uq'_x = f w'_z.} \tag{8.42}$$

This is a single equation for two unknowns (q' and w'), so we need more information (i.e., assumptions) to make a complete theory. The strategy is to approximate both q' and $\hat{w}'_z$ in terms of the pressure perturbation π'.

The Left-Hand Side of (8.42)

We begin with an assumption concerning the perturbation momentum equations (8.15) and (8.16). In each of those equations, it is often true that the individual terms on the right-hand side, i.e., the pressure gradient and the Coriolis acceleration, are large in magnitude compared with the terms on the left-hand side. In other words, the left-hand side is not zero, but it is a small difference of large numbers. It follows that the pressure gradient and Coriolis terms are nearly equal. If those terms are, in fact, equal, the perturbation is in geostrophic balance, and the horizontal velocity components can be represented entirely in terms of the pressure perturbation:

https://doi.org/10.1017/9781108640084.009 Published online by Cambridge University Press

$$u^{(g)} = -\frac{\hat{\pi}'_y}{f}\,; \quad v^{(g)} = \frac{\hat{\pi}'_x}{f}. \tag{8.43}$$

In fact, the horizontal velocity perturbation can be thought of as the sum of a *geostrophic part* and an *ageostrophic part*:

$$u' = u^{(g)} + u^{(a)}\,; \quad v' = v^{(g)} + v^{(a)}.$$

We can do the same with the perturbation vorticity:

$$q' = q^{(g)} + q^{(a)}$$

where the geostrophic part

$$q^{(g)} = v^{(g)}_x - u^{(g)}_y = \frac{1}{f}\nabla^2_H \pi'.$$

Our assumption is that the ageostrophic part is negligible, i.e., $|q^{(a)}| \ll |q^{(g)}|$, so that

$$q' = \frac{1}{f}\nabla^2_H \pi'. \tag{8.44}$$

The Right-Hand Side of (8.42)

Suppose we try to approximate w'_z in the same way, by assuming that it is dominated by its geostrophic part. From continuity we have

$$\begin{aligned} w'_z = -(u'_x + v'_y) &= -(u^{(g)}_x + u^{(a)}_x + v^{(g)}_y + v^{(a)}_y) \\ &= -\left(-\frac{\pi'_{yx}}{f} + u^{(a)}_x + \frac{\pi'_{xy}}{f} + v^{(a)}_y\right) \\ &= -(u^{(a)}_x + v^{(a)}_y). \end{aligned}$$

So, we cannot assume that the ageostrophic part of w'_z is negligible because it's the only part (the geostrophic part being zero). Instead, we invoke the buoyancy equation (8.10), which we write in the form

$$B_z w' = -B_y v' - b'_t - U b'_x. \tag{8.45}$$

We assume once again that v' is dominated by its geostrophic part $v^{(g)}$, and moreover that the perturbation is in hydrostatic balance $b' = \pi'_z$. Making the appropriate substitutions, (8.45) becomes

$$B_z w' = -\frac{B_y}{f}\pi'_x - \pi'_{zt} - U\pi'_{zx} \tag{8.46}$$

and, after a differentiation,

$$B_z w'_z = -\frac{B_y}{f}\pi'_{xz} - \pi'_{zzt} - U\pi'_{zzx} - U_z\pi'_{zx}.$$

https://doi.org/10.1017/9781108640084.009 Published online by Cambridge University Press

Remembering the thermal wind balance $fU_z = -B_y$, we see that the first and last terms on the right-hand side cancel, and therefore

$$w'_z = -\frac{1}{B_z}(\pi'_{zzt} - U\pi'_{zzx}). \tag{8.47}$$

With (8.47) and (8.44), we have accomplished our goal of approximating both q' and $\hat{w}'_z$ in terms of π'.

The Potential Vorticity Equation

Inserting (8.47) and (8.44) into (8.42), we have

$$\xi'_t + U\xi'_x = 0, \tag{8.48}$$

where ξ' is the linearized, quasigeostrophic potential vorticity

$$\boxed{\xi' = \nabla_H^2\pi' + \frac{f^2}{B_z}\pi'_{zz}.} \tag{8.49}$$

Equation (8.48) states that, to an observer moving with the mean along-front current U, the potential vorticity of the perturbation remains constant. If the perturbation is in fact growing exponentially, then its potential vorticity can have only one value and that value is zero.

We next reconfigure (8.48, 8.49) so that it can be solved in a finite vertical domain with impermeable upper and lower boundaries. We assume that π' has the normal mode form

$$\pi' = \hat{\pi}(z)e^{\iota k(x-ct)+\iota\ell y},$$

and similarly for ξ'. Equation (8.48) becomes

$$\iota k(U-c)\hat{\xi} = 0$$

or, as anticipated, $\hat{\xi} = 0$ for $c \neq 0$. From (8.49) we now obtain an ordinary differential equation

$$\boxed{\hat{\pi}_{zz} - \mu^2\hat{\pi} = 0,} \tag{8.50}$$

where

$$\mu = \frac{\tilde{k}}{P} \tag{8.51}$$

is a scaled vertical wavenumber. The Prandtl ratio P is defined as

$$P = \frac{|f|}{\sqrt{B_z}}, \tag{8.52}$$

and $\tilde{k}^2 = k^2 + \ell^2$ as usual.

https://doi.org/10.1017/9781108640084.009 Published online by Cambridge University Press

The Impermeable Boundary Condition

We must now express the boundary condition $\hat{w} = 0$ in terms of $\hat{\pi}$. To this end we write (8.46) in the normal mode form

$$B_z \hat{w} = -\frac{B_y}{f} \imath k \hat{\pi} - \imath k (U - c) \hat{\pi}_z,$$

or, invoking thermal wind balance $B_y = -f U_z$,

$$B_z \hat{w} = \imath k [U_z \, \hat{\pi} - (U - c) \hat{\pi}_z].$$

The boundary condition $\hat{w} = 0$ is therefore equivalent to

$$\boxed{(U - c) \hat{\pi}_z - U_z \hat{\pi} = 0.} \tag{8.53}$$

8.7.2 Eady Waves

We can solve (8.50) with (8.53) imposed at upper and lower boundaries, or with one boundary at infinity. In the latter case, the solution describes Eady waves, which are analogous to the vorticity waves discussed in section 3.12.2. And, like the vorticity waves, a pair of Eady waves can resonate to drive exponential growth.

Before deriving the Eady wave dispersion relation, we give a qualitative description of the mechanism. In Figure 8.5a, we are looking across a frontal zone from the warm (buoyant) side, shaded in red. Now consider an imaginary horizontal surface, and suppose that the fluid is displaced upward and downward by some means so that the surface varies sinusoidally in the along-front direction. At the top of the domain is an impenetrable horizontal boundary where the amplitude of the displacement must decrease to zero as shown by the thin curves.

Because the vertical motion drops to zero at the boundary, the fluid above each trough of the perturbation experiences an extensional strain, $w'_z > 0$, which stretches, and thereby amplifies, the ambient vorticity f. The result is a counterclockwise increment of vorticity as shown at the top of Figure 8.5b by the curved arrows. In contrast, the strain above each crest is compressive, effectively reducing the ambient vorticity, so that the increment is clockwise. Between these strips of oppositely signed vorticity increments are cross-front currents that carry alternately dense (blue) and buoyant (red) fluid.

In each cross-front current, gravity acts to accelerate the fluid vertically: upward in buoyant currents, downward in dense currents (Figure 8.5c). As a result, the nodes of the sinusoidal disturbance are displaced vertically such that the whole pattern propagates to the left.

This intrinsic leftward propagation is relative to the mean along-front current, which must be rightward to maintain thermal wind balance. At the *lower* boundary,

https://doi.org/10.1017/9781108640084.009 Published online by Cambridge University Press

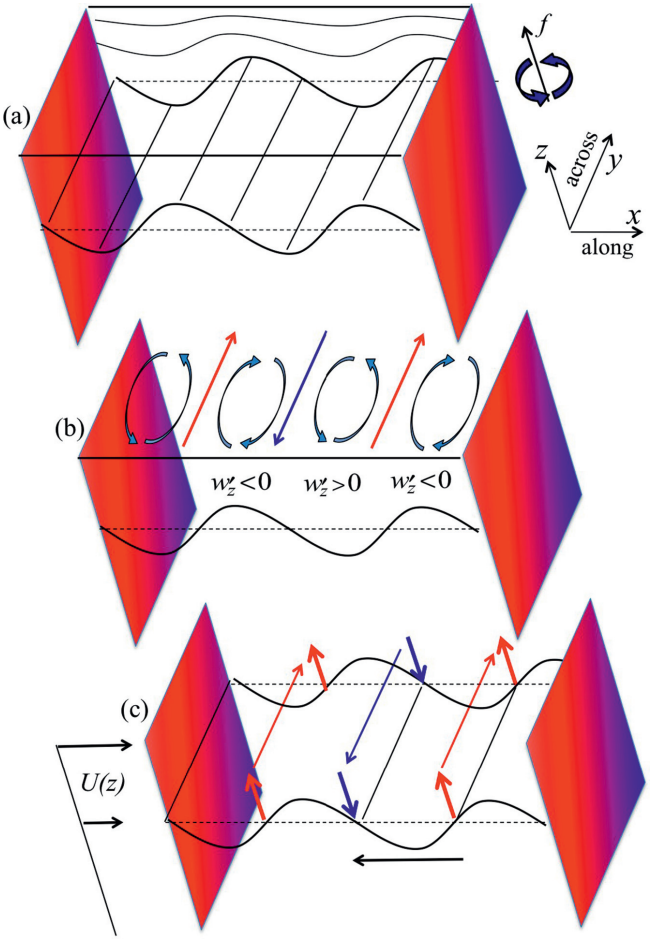

Figure 8.5 Mechanics of Eady wave propagation. (a) Sinusoidal perturbation of a frontal zone in thermal wind balance. Shading on the cross-sections indicates the mean buoyancy distribution: dense (blue) and buoyant (red). The figure assumes $f > 0$, i.e., that we are in the northern hemisphere. (b) Circulations induced by stretching and compression of the ambient vorticity, and the resulting cross-front circulations. (c) Advected buoyancy drives rising and sinking motions, which cause the pattern to propagate to the left, counter to the mean along-front flow U.

the same dynamic supports a right-going wave in a leftward background current. It is therefore possible for both waves to be stationary and, if their relative phases are such that the vertical motion of one wave reinforces the crests and troughs of the other, positive feedback leads to a growing instability, just as we saw with vorticity waves in Chapter 3 (Figure 3.23).

https://doi.org/10.1017/9781108640084.009 Published online by Cambridge University Press

To derive a dispersion relation for the Eady wave shown in Figure 8.5, we solve (8.50), with (8.53) imposed at the upper boundary and the condition that the solution remain bounded as $z \to -\infty$. The general solution of (8.50) is

$$\hat{\pi} = \alpha e^{\mu z} + \beta e^{-\mu z}, \tag{8.54}$$

where α and β are constants. Boundedness as $z \to -\infty$ requires that $\beta = 0$. In this case $\hat{\pi}_z = \mu\hat{\pi}$, and the boundary condition becomes

$$(U_u - c)\mu - U_z = 0,$$

where U_u is the mean along-front velocity at the boundary. Solving for c, we have

$$c = U_u - \frac{U_z}{\mu}. \tag{8.55}$$

For a wave at a lower boundary, we carry out the same steps, this time requiring boundedness as $z \to +\infty$. In this case $\alpha = 0$, $\hat{w}_z = -\mu\hat{w}$, and the boundary condition gives the dispersion relation

$$c = U_l + \frac{U_z}{\mu}, \tag{8.56}$$

where U_l is the mean along-front velocity at the lower boundary.

The upper and lower waves propagate oppositely relative to the mean flow at their respective boundaries. It is therefore possible that their phase speeds could be equal. In that case, the two waves might resonate and drive exponential growth. To see if this possibility is in fact true, we must solve (8.50) with (8.53) imposed at both the upper and lower boundaries.

8.7.3 The Eady Mode of Baroclinic Instability

We consider a finite domain, with coordinates chosen such that boundaries are at $z = \pm H/2$ and the mean along-front velocity is $U = U_z z$. The general solution of (8.54) must satisfy the boundary conditions

$$\left(-\frac{U_z H}{2} - c\right)\hat{\pi}_z + U_z\hat{\pi} = 0 \quad \text{at } z = -\frac{H}{2}$$

and

$$\left(\frac{U_z H}{2} - c\right)\hat{\pi}_z + U_z\hat{\pi} = 0 \quad \text{at } z = \frac{H}{2}.$$

https://doi.org/10.1017/9781108640084.009 Published online by Cambridge University Press

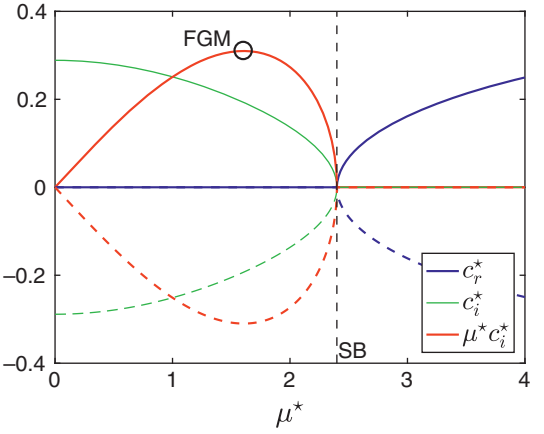

Figure 8.6 Phase speed (real = blue, imaginary = green) and scaled growth rate $\mu^\star c_i^\star$ (red) versus vertical length scale for the Eady model of baroclinic instability, based on (8.57). Scalings are defined by $\mu^\star = \mu H$ and $c^\star = c/U_z H$. Annotations mark the fastest-growing mode (FGM) and the stability boundary (SB).

Substituting (8.54) and solving for c, we obtain

$$\boxed{c^{\star 2} = \frac{1}{4} - \frac{\coth \mu^\star}{\mu^\star} + \frac{1}{\mu^{\star 2}},} \tag{8.57}$$

where the nondimensional phase speed and vertical scale are

$$c^\star = \frac{c}{U_z H}\,; \quad \mu^\star = \mu H. \tag{8.58}$$

The solution (8.57) is shown in Figure 8.6. For $\mu^\star > 2.40$, c is real and represents oppositely propagating modes. In the limit $\mu^\star \to \infty$ (in which the domain height is large compared to the vertical scale μ^{-1}), these correspond to the isolated Eady waves described in section 8.7.2.[6]

As $\mu^\star$ decreases from infinity, the two Eady waves become close in phase speed. At $\mu^\star = 2.40$, both phase speeds reach zero, i.e., the waves become phase locked.

[6] For $\mu^\star \gg 1$, $\coth \mu^\star$ approaches 1. Therefore,

$$c^{\star 2} \approx \frac{1}{4} - \frac{1}{\mu^\star} + \frac{1}{\mu^{\star 2}} = \left(\frac{1}{2} - \frac{1}{\mu^{\star 2}}\right)^2.$$

In dimensional terms,

$$c \approx \pm\left(\frac{U_z H}{2} - \frac{U_z}{\mu}\right),$$

which is equivalent to the dispersion relations (8.55, 8.56) for the upper and lower Eady waves derived in section 8.7.2.

https://doi.org/10.1017/9781108640084.009 Published online by Cambridge University Press

For $\mu^\star < 2.40$, c is imaginary and we therefore have unstable modes with real growth rate σ. The growth rate is proportional to the product $\mu^\star c_i^\star$:

$$\sigma = kc_i = \frac{k}{\tilde{k}}\,\tilde{k}\,c_i^\star U_z H = \frac{k}{\tilde{k}}\,\frac{\mu}{P}\,c_i^\star U_z H = \frac{k}{\tilde{k}}\,\frac{U_z}{P}\,\mu^\star c_i^\star, \tag{8.59}$$

where (8.51) and (8.58) have been used.

Instead of oppositely propagating waves, the solutions represent one growing and one decaying mode (Figure 8.6). The product $\mu^\star c_i^\star$ reaches a maximum of 0.31 at $\mu^\star = 1.61$ (circle on Figure 8.6), then drops to zero at $\mu^\star = 0$. This band of unstable modes $0 < \mu^\star \le 2.40$ is the Eady mode of baroclinic instability, which we will call the Eady mode for short.

We will be most interested in the fastest-growing Eady mode. The optimal nondimensional length scale $\mu^\star = 1.61$ corresponds to

$$\tilde{k} = \frac{1.61}{H} P. \tag{8.60}$$

The wavelength is

$$\lambda = \frac{2\pi}{\tilde{k}} = \frac{3.9}{P} H.$$

This is sometimes written as

$$\lambda = 3.9 L_d,$$

where

$$L_d = \frac{H}{P}$$

is called the deformation radius.

For the optimal value of $\mu^\star$, the dimensional growth rate is given by (8.59):

$$\sigma = 0.31\,\frac{k}{\tilde{k}}\,P\,U_z.$$

Like shear instability, the Eady mode grows fastest when $k = \tilde{k}$, or $\ell = 0$, i.e., when the wave vector is aligned with the mean along-front flow. The maximum growth rate is then proportional to the thermal wind shear and also to the Prandtl ratio:

$$\sigma = 0.31\,P\,U_z. \tag{8.61}$$

There are two interesting alternative ways to express this growth rate. First:

$$\sigma = 0.31\,\sqrt{B_z}\,s_b,$$

https://doi.org/10.1017/9781108640084.009 Published online by Cambridge University Press

i.e., the growth rate depends on the strength of the stratification and the degree to which the isopycnals are tilted. Second:

$$\sigma = 0.31 \frac{|f|}{\sqrt{Ri}}. \tag{8.62}$$

8.7.4 Terrestrial Examples

The Prandtl ratio

We now look at some typical dimensional parameter values for baroclinic instability, beginning with the Prandtl ratio $f/\sqrt{B_z}$. A typical mid-latitude value for f is 10^{-4}s^{-1} (section 1.5). In the troposphere, a typical value for B_z is 10^{-4}s^{-2}. Coincidentally, this value is also typical of the upper ocean. Therefore, the Prandtl ratio is near 0.01 in both fluids.

The Prandtl ratio exerts a control on the aspect ratio (i.e., the height to length ratio) of the eddy structures that result from baroclinic instability. This is in line with the wave length scaling in (8.60) above, which states that $H/\lambda \propto f/\sqrt{B_z}$. An illustration of this feature can be seen in Figure 8.7, where mesoscale eddies, thought to arise from baroclinic instability, have been observed from a mooring that measures the horizontal velocity of the upper 2000 m of the Arctic Ocean from a position fixed to the sea bed. The sudden bursts of enhanced horizontal velocity indicate the passage of eddies at various depths over a number of years. Due to the strong stratification in the upper 200 m, the Prandtl ratio confines the shallower eddies in this region to small vertical scales. This is not the case in the deeper (> 200 m) ocean, where the much weaker stratification allows the eddies to extend thousands of meters in the vertical. Notice that some eddies also have cores

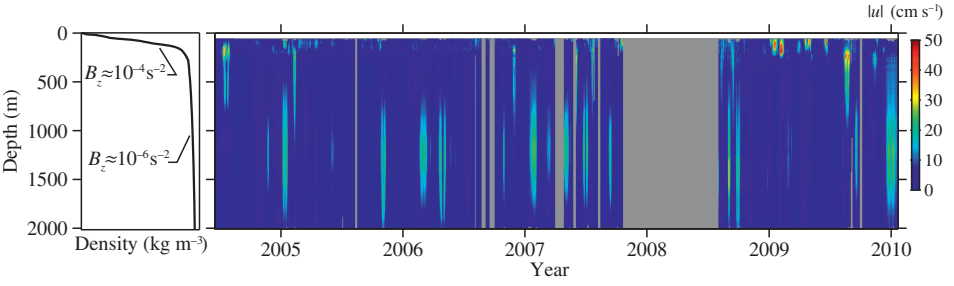

Figure 8.7 Observations of horizontal velocity magnitude from a mooring in the Arctic Ocean together with a representative density profile (left). The different vertical signatures of the eddies illustrate the dependence of the vertical scale height to the Prandtl ratio, $f/\sqrt{B_z}$, which changes by an order of magnitude. The horizontal scale of the eddies varies between 10 and 40 km [adapted from Carpenter and Timmermans (2012), see also Zhao and Timmermans (2015)].

https://doi.org/10.1017/9781108640084.009 Published online by Cambridge University Press

that are centered at the transition between the two different stratification regimes so that they have very asymmetrical velocity signatures – being able to extend to great depths once they are able to "puncture" through to the weakly stratified layer.

The troposphere: If we take H to be the atmospheric scale height, which is near 10 km, then the deformation radius is 1000 km and the wavelength of the fastest-growing Eady mode is about 4000 km. Now suppose that the wind speed changes by 10 m/s over the scale height H, so that $U_z = 10^{-3}\text{s}^{-1}$. The growth rate is then $3 \times 10^{-6}\text{s}^{-1}$, for an e-folding time of 4 days. These estimates are "in the ballpark" for mid-latitude weather systems, which develop over a few days and have longitudinal extents of a few thousand kilometers.

The ocean thermocline: In the ocean, the depth over which baroclinic instability acts is more like 1 km, so the predicted wavelength is 1/10 of the atmospheric value, say 400 km. This is a typical length scale for mesoscale eddies. If the current changes by 0.1 m/s over 1 km depth, then U_z is 10^{-4}s^{-1}, and the predicted e-folding time is about a month, not too different from the time scale for mesoscale eddy growth.

The ocean mixed layer: The upper few tens of meters of the ocean is well mixed by wind and waves. But while buoyancy and other properties vary little in the vertical, they can vary substantially in the horizontal. The result is a class of baroclinic and symmetric instabilities that currently goes by the general name *mixed layer instability* (Boccaletti et al., 2007). Because stratification is weak, the Prandtl ratio is relatively large, $P = 0.1$ perhaps. The depth of the layer is of order 100 m, so the Eady model predicts a wavelength of 4 km, in the *submesoscale* range. If we assume a velocity scale of 0.1 m/s, we get an e-folding time of 9 hours.

8.8 Numerical Solution Method

Numerical solution of (8.8–8.10) is more complicated than in the non-rotating cases we have studied previously for two main reasons:

(1) elimination of the pressure is harder because the pressure equation acquires a Coriolis term, and
(2) the variation of the background state in both y and z complicates the application of normal modes.

In the analytic solutions above we sidestepped those problems by making various assumptions (no variation in x for inertial and symmetric instabilities, the quasi-geostrophic approximation for the Eady mode). Numerical methods allow us to relax those assumptions, at least in part. In what follows we will describe the two problems in turn, and then describe the solution.

https://doi.org/10.1017/9781108640084.009 Published online by Cambridge University Press

8.8.1 The Pressure Equation

Taking the divergence of (8.9) gives the pressure equation

$$\nabla^2 \pi' = -2U_y \frac{\partial v'}{\partial x} - 2U_z \frac{\partial w'}{\partial x} + \frac{\partial b'}{\partial z} + f\left(\frac{\partial v'}{\partial x} - \frac{\partial u'}{\partial y}\right). \tag{8.63}$$

With $f \neq 0$, u' and v' appear on the right-hand side, hence our usual tactic of using the pressure equation to eliminate those variables will have to be reconsidered.

8.8.2 Limitations of the Normal Mode Approach

To solve the perturbation equations (8.1, 8.9, 8.10) we assume solutions of the form

$$u' = \hat{u}(z) e^{\sigma t} e^{\iota(kx+\ell y)}. \tag{8.64}$$

This requires that the coefficients depend only on z.

Now consider the second terms in (8.9) and (8.10). These describe advection of the perturbation by the background flow, and have the form U times $\partial/\partial x$ of something. If the perturbation is independent of x, as in the inertial and symmetric instabilities (section 8.6), those terms vanish regardless of the form of U. For a general perturbation, however, the factor U must depend only on z, i.e.,

$$U_y = 0. \tag{8.65}$$

In addition, thermal wind balance requires that $B_{yy} = f U_{yz} = 0$, hence

$$B = B_y y + \vartheta(z), \tag{8.66}$$

where B_y is a constant and ϑ is an arbitrary function.

8.8.3 Reduction to an Eigenvalue Problem

With the constraints (8.66) and (8.65) satisfied, we substitute (8.64) into (8.8–8.10) to obtain the normal mode perturbation equations

$$\iota k\hat{u} + \iota\ell\hat{v} + \hat{w}_z = 0 \tag{8.67}$$

$$(\sigma + \iota kU)\hat{u} + U_z\hat{w} = -\iota k\hat{\pi} + f\hat{v} \tag{8.68}$$

$$(\sigma + \iota kU)\hat{v} = -\iota\ell\hat{\pi} - f\hat{u} \tag{8.69}$$

$$(\sigma + \iota kU)\hat{w} = -\hat{\pi}_z + \hat{b} \tag{8.70}$$

$$(\sigma + \iota kU)\hat{b} + B_y\hat{v} + \vartheta_z\hat{w} = 0. \tag{8.71}$$

Instead of using $\hat{u}$ and $\hat{v}$, we define new variables

$$\hat{q} = \iota k\hat{v} - \iota\ell\hat{u}\,; \quad \hat{\chi} = \iota k\hat{u} + \iota\ell\hat{v}. \tag{8.72}$$

https://doi.org/10.1017/9781108640084.009 Published online by Cambridge University Press

The first of these is just the normal mode form of the perturbation vertical vorticity defined in section 8.5. Its evolution equation, arrived at by cross-differentiating (8.68) and (8.69), is

$$(\sigma + \imath kU)\hat{q} - \imath \ell U_z \hat{w} = f\hat{w}_z. \tag{8.73}$$

This is the normal mode form of (8.17). [The limitation $U_y = 0$ has been imposed in accordance with (8.65), so that y-derivatives of U vanish and $f_a = f$.]

Our next goal is to eliminate $\hat{\pi}$ from the vertical momentum equation (8.70). The troublesome pressure equation (8.63) can be written as

$$\nabla^2 \hat{\pi} = -2\imath kU_z \hat{w} + \hat{b}_z + f\hat{q} \tag{8.74}$$

where, as usual,

$$\nabla^2 = \frac{d^2}{dz^2} - \tilde{k}^2 \,, \quad \text{and } \tilde{k} = \sqrt{k^2 + \ell^2}.$$

In section 3.1.2, we discussed in detail the procedure of eliminating pressure by (1) deriving a Poisson equation like the one above, (2) taking the Laplacian of the vertical velocity equation, and combining the two. Thanks to our use of $\hat{q}$, that procedure will work here. Starting with (8.70) and applying ∇^2, we obtain

$$(\sigma + \imath kU)\nabla^2 \hat{w} + 2\imath kU_z \hat{w}_z = -\nabla^2 \hat{\pi}_z + \nabla^2 \hat{b},$$

remembering that $U_{zz} = 0$. Differentiating (8.74) and substituting leads, after some gratifying cancellations, to

$$(\sigma + \imath kU)\nabla^2 \hat{w} = -\tilde{k}^2 \hat{b} - f\hat{q}_z. \tag{8.75}$$

In (8.73) and (8.75) we have two equations for the three unknown functions $\hat{q}$, $\hat{w}$, and $\hat{b}$. To close the system we will add the buoyancy equation (8.71), but note that (8.71) involves dependence on $\hat{v}$. To remove this dependence, we solve the pair of equations (8.72) for $\hat{v}$:

$$\hat{v} = -\frac{\imath k}{\tilde{k}^2}\hat{q} - \frac{\imath \ell}{\tilde{k}^2}\hat{\chi},$$

and remember that $\hat{\chi} = -\hat{w}_z$ by (8.67). With this substitution, (8.71) becomes

$$(\sigma + \imath kU)\tilde{k}^2 \hat{b} = \imath k B_y \hat{q} - \imath \ell B_y \hat{w}_z - \tilde{k}^2 \vartheta_z \hat{w}. \tag{8.76}$$

> Exercise: Compare (8.75, 8.76) with (4.14, 4.15) and also with (6.14, 6.15). Note all differences, and make sure you can explain each in terms of the different assumptions that have been made.

https://doi.org/10.1017/9781108640084.009 Published online by Cambridge University Press

We now have three equations, (8.73), (8.75), and (8.76) for the three unknowns $\hat{q}$, $\hat{w}$, and $\hat{b}$, which we can write as a matrix differential equation:

$$\sigma \begin{pmatrix} 1 & 0 & 0 \\ 0 & \nabla^2 & 0 \\ 0 & 0 & 1 \end{pmatrix} \begin{pmatrix} \hat{q} \\ \hat{w} \\ \hat{b} \end{pmatrix} = \begin{pmatrix} -\imath k U & \imath \ell U_z + f D^{(1w)} & 0 \\ -f D^{(1q)} & -\imath k U \nabla^2 & -\tilde{k}^2 \\ \dfrac{\imath k}{\tilde{k}^2} B_y & -\dfrac{\imath \ell}{\tilde{k}^2} B_y D^{(1w)} - \vartheta_z & -\imath k U \end{pmatrix} \begin{pmatrix} \hat{q} \\ \hat{w} \\ \hat{b} \end{pmatrix}, \tag{8.77}$$

with

$$\nabla^2 = D^{(2)} - \tilde{k}^2$$

and

$$D^{(1)} = \frac{d}{dz}; \quad D^{(2)} = \frac{d^2}{dz^2}.$$

The first-derivative operators in (8.77) are marked with the superscripts w and q to indicate that their matrix equivalents may be different depending on the choice of boundary conditions (see below). We now replace the derivative operators $D^{(1)}$ and $D^{(2)}$ with derivative matrices as defined previously (sections 1.4.2, 3.5, 5.5, and 6.2), remembering to incorporate the appropriate boundary conditions. The result is a generalized eigenvalue problem with $3N \times 3N$ matrices:

$$\sigma\, \mathsf{A}\vec{x} = \mathsf{B}\vec{x}.$$

The eigenvector $\vec{x}$ is a concatenation of the discretized forms of $\hat{q}$, $\hat{w}$, and $\hat{b}$.

8.8.4 Boundary Conditions

For $\hat{w}$, we use the impermeable boundary $\hat{w} = 0$. Application of this boundary condition should be familiar by now. For buoyancy, (8.77) does not require a boundary condition since $\hat{b}$ is not differentiated.

The new variable is the vertical vorticity q. Differentiating the definition (8.14), we have

$$\frac{\partial q'}{\partial z} = \frac{\partial}{\partial z}\left(\frac{\partial v'}{\partial x} - \frac{\partial u'}{\partial y}\right) = \frac{\partial}{\partial x}\frac{\partial v'}{\partial z} - \frac{\partial}{\partial y}\frac{\partial u'}{\partial z}. \tag{8.78}$$

If we now assume that the boundary is *frictionless*, as described in section 5.4.2, then this reduces to $\partial q'/\partial z = 0$ or, in normal mode form,

$$\hat{q}_z = 0.$$

We now need a first-derivative matrix for $\hat{q}$ that incorporates this boundary condition. The necessary modifications are derived in section 5.5; the top and bottom rows are $[-2/3 \;\; 2/3 \;\; \ldots]/\Delta$ and $[\ldots \;\; 2/3 \;\; -2/3]/\Delta$.

https://doi.org/10.1017/9781108640084.009 Published online by Cambridge University Press

8.8.5 Shear Scaling

Suppose that (8.77) has a solution algorithm:

$$[\sigma, \hat{q}, \hat{w}, \hat{b}] = \mathcal{F}(z, U_z, \vartheta_z, f;\ k, \ell).$$

Now let us choose the time scale to be $1/U_z$ and the length scale to be the domain height H. The nondimensionalization is straightforward. Scalings of particular interest are

$$f^\star = \frac{f}{U_z},$$

and

$$\vartheta^\star_{z^\star} = \frac{\vartheta_z}{U_z^2} = Ri(z),$$

the gradient Richardson number. Note that Ri can vary with height.

The scaled equations are isomorphic to (8.77), and therefore

$$[\sigma^\star, \hat{q}^\star, \hat{w}^\star, \hat{b}^\star] = \mathcal{F}(z^\star, 1, Ri(z^\star), f^\star;\ k^\star, \ell^\star).$$

Time scales other than $1/U_z$ are possible, e.g., $1/|f|$. If the stratification ϑ_z has an identifiable "characteristic" value B_z, then $1/\sqrt{B_z}$ is also a viable time scale.

8.9 Instability in the Ageostrophic Regime

Numerical solutions of (8.77) as described above can approximate the analytically derived inertial, symmetric, and baroclinic instabilities (sections 8.6 and 8.7), as well as allowing us to relax some simplifying assumptions for greater realism. In the example shown in Figure 8.8, variables are scaled by the shear and the domain height (see section 8.8.5). We set the Prandtl ratio to the typical terrestrial value $P = 0.01$ and the Richardson number to $Ri = 0.94$. At the largest values of $k^\star$ and $\ell^\star$ (upper right), instabilities are oscillatory, but for smaller wavenumbers (lower left) stationary modes are found.

The symmetric mode is visible at the left, where $k^\star = 0$. Modes with small $\ell^\star$ (and $k^\star = 0$, lower left) are damped in the presence of boundaries, but at large $\ell^\star$ the growth rate is consistent with the analytical solution $P\sqrt{1 - Ri}$. The fastest-growing mode along the bottom edge ($\ell^\star = 0$), indicated by "AB," is a stationary baroclinic instability similar to the Eady mode (section 8.7). For this example Ri has been set close to the value at which the symmetric and baroclinic modes have equal growth rate. For comparison, the symbol "QB" shows the wavenumber $1.61P$, the predicted value for the baroclinic mode in the quasigeostrophic regime $Ri \gg 1$.

https://doi.org/10.1017/9781108640084.009 Published online by Cambridge University Press

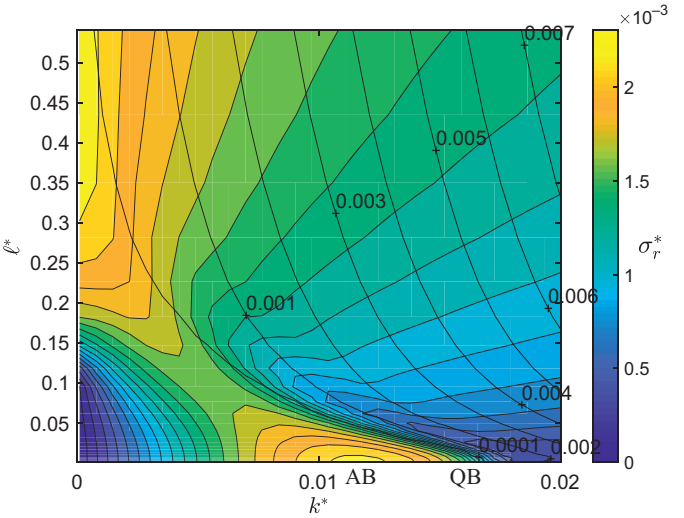

Figure 8.8 Growth rates of instabilities far from the quasigeostrophic regime. All background gradients are uniform. Shear scaling is used, with parameter values $P = 0.01$, $Ri = 0.94$. Filled (plain) contours show the growth rate (frequency). Symbols "AB": ageostrophic baroclinic instability; "QB": quasi-geostrophic (Eady) baroclinic instability. Numerical solution employs $N = 100$ grid points.

Exercise: The student is invited to develop the code and explore the instabilities further. Useful papers for reference are Stone (1966) and Stamper and Taylor (2016).

8.10 Summary

- A stratified fluid in a rotating environment is in equilibrium if the pressure is hydrostatic and the thermal wind balance holds: $fU_z = -B_y$.
- The perturbation equations can be solved numerically after the introduction of the vertical vorticity perturbation.
- Inertial instability
  - Arises from a sheared current in a rotating environment in the absence of stratification.
  - Instability requires that the shear produces a relative vorticity that is greater than, and in opposition to the planetary vorticity, i.e., $|U_y| > |f|$ and $-U_y f > 0$.
  - There is no preferred wavelength, and the motions are purely horizontal.
  - The instability is caused by a continual alignment of the perturbation velocity so that it is able to extract the shear of the equilibrium current.
- Symmetric instability
  - Instability requires $Ri < f_a/f$.

https://doi.org/10.1017/9781108640084.009 Published online by Cambridge University Press

  - Perturbations do not vary in the along-front (x) direction.
  - Motion is along isopycnals in the ($y - z$) plane.
  - There is no preferred wavelength.
  - The physical mechanism of the instability is the same as inertial instability, except it has an additional influence of the vertical shear in the thermal wind equilibrium.
- Baroclinic instability (the Eady model)
  - Flow is assumed to be quasigeostrophic.
  - Perturbations do not vary in the cross-front (y) direction.
  - Motion is sinusoidal, with phase velocity stationary with respect to the central plane.
  - The wavelength $\lambda = 3.9H/P$, where $P = |f|/\sqrt{B_z}$.
  - The growth rate $\sigma = 0.31PU_z = 0.31|f|/\sqrt{Ri}$.
  - The instability can be understood as a resonance of Eady wave trains focused near the upper and lower boundaries.

8.11 Further Reading

Theoretical details are developed further in Pedlosky (1987), Haine and Marshall (1998), and Thomas et al. (2013). For more details of wave resonance in baroclinic instability see Bretherton (1966) and Heifetz et al. (2004).

https://doi.org/10.1017/9781108640084.009 Published online by Cambridge University Press